Spring Loaded Inverted Pendulum (SLIP) Approximate Stance Map For Nonsymmetric Motions and Variable Stiffness

Ömür Arslan

Bilkent University
Electrical & Electronics Engineering Department

July 07, 2008

Abstract

Spring loaded inverted pendulum (SLIP) is frequently used as a fundamental model to analyze and estimate human, animal and robotics locomotions. In general, a locomotion motion is considered in two phases; flight phase , when there is no ground contact, and stance phase , when there is a ground contact. Due to the major difference of the phases (ground contact), dynamics of the model is different. In flight phase, SLIP performs a ballistic flow and it has a well known and analytically solved dynamics. However, due to gravity, stance phase dynamics is much more complicated and it includes nonintegrable terms. Several approximate analytical stance maps are derived by neglecting or approximating gravity effect, especially symmetric gaits are studied since the locomotion converges to symmetric trajectories for a constant desired motions on flat surfaces. On the other hand, humans, animals and robots may need to use various terrains (grass, rock field, etc) to survive. For these environments, converging a symmetric gait may not be possible and intuitively the resultant gaits are always nonsymmetric. Moreover, to locomote on these terrains without any trouble, several control strategies are needed to determine leg touchdown angles and leg stiffness (or touchdown or liftoff leg lengths), which are the control parameters for the SLIP template. Therefore, the approximate stance map for nonsymmetric gaits and variable stiffness case becomes much more valuable to perform motion planning and control of SLIP.

In this report, various gravity effect corrections for angular momentum, named as total virtual gravity effect on angular momentum, are used to improve the performance of previous studies on approximate stance map in which gravity effects are approximated by small angle assumptions. Furthermore, these maps are rearranged for variable stiffness for compression and decompression phases. Finally, several performance analyses are done to examine the results of approximate map with virtual gravity effect corrections and variable stiffness.

Contents

List of Figures

List of Tables

1 Introduction

Intuitively, *legs are better than wheels* and it is obvious because they have wider range of different environment applications. In [5], Raibert summarizes advantages of legged system compared to wheeled one with two reasons. One reason is that mobility of legged systems is considerably better than vehicles with wheels because legged robots can be used in difficult terrains where wheeled systems cannot travel. The second one is that application areas of wheeled vehicles on the world are limited with prepared arenas (e.g roads and rails) and some natural ambulatories. On the other hand, legged robots can reach all the regions that animals can travel on foot. One of the important primary studies on dynamical legged locomotion and balance is done by Raibert. He used a one legged robot modeled as SLIP such that body mass dominates leg and pneumatic leg structure behaves as adjustable spring. He performed several simulations and experiments with different model based control techniques for asymptotically stable locomotion and balance.In summary, Raibert claims in his book that troting motion of a quadruped is similar to a biped locomotion, a biped is similar to a monoped runner and control problem of a monoped is solved[5]. Similarly, Saranli and Koditschek used a model based controller for a hexapedal runner, their lower dimensional model was a passively compliant biped [7].

In both studies, researchers were interested in stable forward running, and these studies are valuable because humans, animals and robots mostly uses forward locomotions but not *always* . Especially, due to some critical events (e.g. an obstacle or critical power level) stopping and backward locomotions can be desired. To perform these motions in a safely manner, different new model based control algorithms are needed, so more accurate state maps are necessary. Since any legged robot can be modeled with a monoped runner, the simplest model, the analytical stance map of a monoped runner is indispensable for real time application. However, Poincaré and Whittacker showed that the stance dynamics of SLIP includes non-integrable terms [4], [12]. Thus, several approximations and assumptions are done to derive the approximate stance map for a monoped runner. One of the common assumption is ignoring gravitational force, and the resultant dynamics becomes completely integrable, but the performance of approximate map is not suitable for large sweep angles. Geyer et al. have introduced another approximate stance map assuming small sweep angle, small spring compression and constant angular momentum during stance phase and

the approximate map has significant performance[3]. Also, Schwind and Koditschek derived another approximate iterative stance map for a monoped runner by using mean value theorem such that the performance of method is improved by increasing iteration number [10].

Organization of the report begins with SLIP model and terminology. Secondly, the details of these two approximation is given in Previous Studies section.Thirdly, proposed virtual gravity effect corrections methods are introduced. Fourthly, application of these stance map approximations and gravity corrections to variable stiffness case is derived. In the following section, performance analysis and compression on approximations is done. Finally, the study is summarized and a conclusion is drawn with the open research topics.

2 SLIP Model

2.1 SLIP Template

Spring loaded inverted pendulum (SLIP) is the simplest and fundamental template to analyze dynamical locomotion of humans, animals and robots from biomechanics and robotics perspectives. This model consists of a point mass that represents the total mass of analyzed object located at the center of mass and a massless complaint leg. During the stance phase, no slippage is assumed so when toe of the leg touches the ground, there is assumed to be a frictionless revolute joint until the liftoff event occurs. In Figure 1, SLIP template and illustration of a human runner with SLIP is presented.

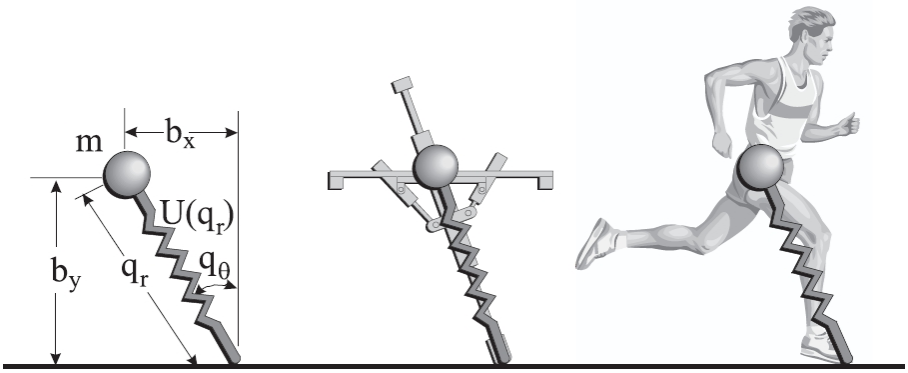

Figure 1: Left:SLIP template - the parameters are defined in notation table. Middle: Raibert's hopper template. Right:SLIP template illustration on a humer runner. This figure is taken from [10].

SLIP is a hybrid systems such that its continuous dynamics changes depending on the ground contact. Based on ground contact, two main phases are defined to analyze slip motion; stance and flight phases. Moreover, each of these two phases are also divided into the two subphases based on sign of rate of change of leg length for stance phase and sign of vertical velocity for flight phase. Also, the transition between these subphases have special properties and importance to determine the locomotion characteristics. Figure 2 shows a single stride started from an apex position and labels show the phases, subphases and transition events. Now, let us give their definitions and general properties.

Flight Phase : A period in which SLIP doesn't touch ground and it performs ballis-

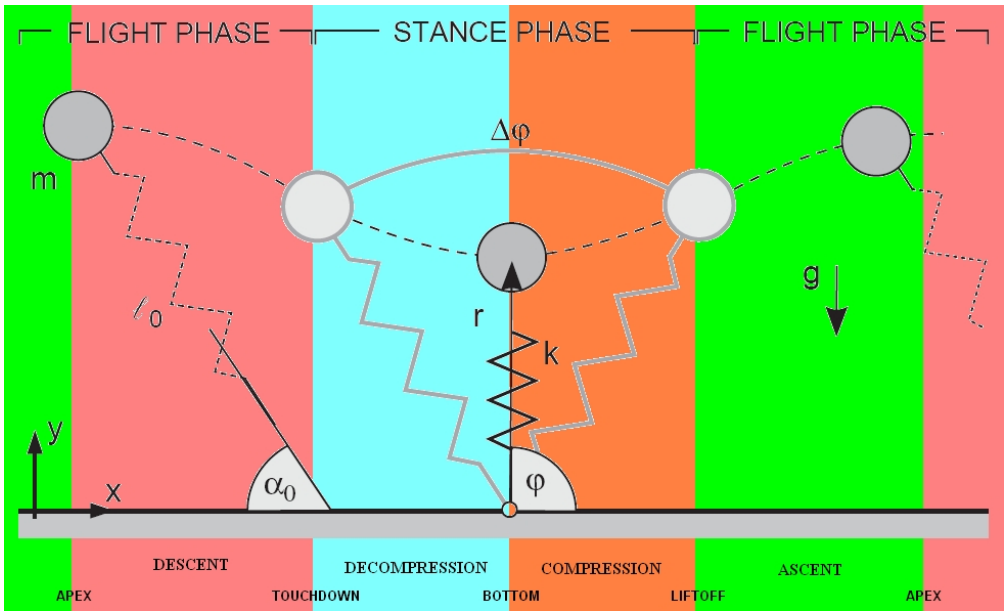

Figure 2: SLIP Model. Locomotion phases, subphases and transition events. This figure is taken from [3].

tic flow which has a well known dynamics. Depending on the vertical velocity, this phase is divided into two subphases; ascent and descent.

Ascent Phase : A subperiod of flight phase such that the vertical velocity is positive (upward) and decreasing in magnitude. In this phase, potential energy due to gravity increases.

Descent Phase : A subperiod of flight phase such that the vertical velocity is negative (downward) and increases in magnitude. In this phase, potential energy due to gravity decreases.

Stance Phase : A period in which the model touches ground. Due to gravitational force, stance phase dynamics consists of non-integrable terms. Also,depending on the rate of change of leg length, this phase is divided into two subphases; compression ans decompression.

Compression Phase : A subperiod of stance phase such that the rate of change of leg length is *negative*. In this phase the stored energy on compliant leg increases.

Decompression Phase : A subperiod of stance phase such that the rate of

change of leg length is *positive*. In this phase the stored energy on compliant leg decreases.

Transition Events : Since our model is a hybrid system, it includes continuous and discrete dynamics. These transition events are boundaries between the phases. To perform a simulation study, the transitions events should be checked. Moreover, these transition events have special meanings; for example, maximum height or minimum leg length are reached during these events. Now, lets give the general properties of these events.

Apex : This event occurs during flight phase between ascent and descent subphases. Also at the instance of this event ,SLIP reaches the maximum height (or maximum gravitational potential energy). To check this event, vertical velocity can be used such that it will be zero.

"Apex occurs if $b_{\dot{y}} = 0$ and SLIP is in flight phase."

Touchdown : Flight phase to stance phase transition event. It occurs when the leg length is equal to touchdown leg length and SLIP descents. To check this event,

"Touchdown occurs if $q_r = q_{r_{td}}$ and $b_{\dot{y}} < 0$ "

Bottom : This event occurs during stance phase between compression and decompression subphases. Also at the instance of this event, spring potential energy reaches maximum (or minimum leg length is reached). To check this event, rate of change of leg length can be used such that it will be zero.

"Bottom occurs if $q_{\dot{r}} = 0$ and SLIP is in stance phase."

Liftoff : Stance phase to flight phase transition event. It occurs when the leg length is equal to liftoff length and SLIP ascents. To check this event,

"Liftoff occurs if $q_r = q_{r_{lo}}$ and $b_{\dot{y}} > 0$ "

Notation used throught the report is listed on Table 1. The result of the previous studies are derived with different notation, to see the original studies look at [3] and [10].

2.2 SLIP Dynamics

As previously stated, SLIP is a hybrid systems, therefore the stance and flight phase dynamics must be separately considered. In this part a general dynamics relations will be provided in cartesian and polar coordinates for simulation studies. The SLIP dynamics for referred previous studies is mentioned in the next section. We will begin with the stance map for general purpose studies.

2.2.1 Stance Dynamics

One of the assumption for the SLIP model is that there is no slippage during the stance phase and so polar coordinate is one of the suitable coordinate system to model the stance dynamics. Therefore, our state vector is

$$\mathbf{q} = \begin{bmatrix} q_\theta \\ q_{\dot{\theta}} \\ q_r \\ q_{\dot{r}} \end{bmatrix}$$

and the stance dynamics is

$$\dot{\mathbf{q}} = \begin{bmatrix} \dot{q}_\theta \\ \dot{q}_{\dot{\theta}} \\ \dot{q}_r \\ \dot{q}_{\dot{r}} \end{bmatrix} = \begin{bmatrix} q_{\dot{\theta}} \\ -\frac{g_s \sin(q_\theta)}{q_r} - \frac{2 q_{\dot{r}} q_{\dot{\theta}}}{q_r} \\ q_{\dot{r}} \\ \frac{F_s(q_r, q_{\dot{r}})}{m} + q_r q_{\dot{\theta}}^2 - g_s \cos(q_\theta) \end{bmatrix}$$

where $F_s(q_r)$ is the spring force function defined according to rest leg length, current leg length and the phase of the locomotion as (also see (2) and (3) for stance dynamics derivation)

$$F_s(q_r, q_{\dot{r}}) = \begin{cases} k_c(l_0 - q_r) & \text{, if } q_{\dot{r}} \leq 0; \\ k_d(l_0 - q_r) & \text{, if } q_{\dot{r}} > 0. \end{cases}$$

Leg & Body Coordinates	
q_r	Leg Length
q_θ	Leg angle from Vertical (counterclockwise convention)
$q_{\dot{r}}$	Leg Compression rate
$q_{\dot{\theta}}$	Leg Swing rate
p_r	Radial Momentum
p_θ	Angular Momentum
b_x	Horizontal Position of Body
b_y	Vertical Position of Body
$b_{\dot{x}}$	Horizontal Velocity of Body
$b_{\dot{y}}$	Vertical Velocity of Body
p_x	Horizontal Momentum
p_y	Vertical Momentum
b_{tx}	Horizontal Position of Toe
SLIP Parameters	
m	Body Mass
l_0	Rest Length of Springy Leg
k	Spring Constant used for general formulization
k_c	Compression Phase Spring Constant
k_d	Decompression Phase Spring Constant
g_s	Gravitational Acceleration during stance phase(positive)
g_f	Gravitational Acceleration during flight phase(positive)
$F_g(x)$	Ground function. For a given position x, it returns the ground height.
$F_s(r, \dot{r})$	Spring force function. For a given leg length it returns spring force based on the stance phase of SLIP.
$U_s(r, \dot{r})$	Spring potential energy function. For a given leg length it returns stored energy on compliant leg based on the stance phase of SLIP.
E	Total Mechanical Energy
Touchdown Parameters	
$q_{\theta_{td}}$	Leg Angle at Touchdown
$q_{r_{td}}$	Leg Length at Touchdown
Liftoff Parameters	
$q_{\theta_{lo}}$	Leg Angle at Liftoff
$q_{r_{lo}}$	Leg Length at Liftoff
Apex Parameters	
$b_{\dot{x}_a}$	Apex Velocity
b_{y_a}	Apex Height

Table 1: Notation for SLIP Template

Similarly, the state vector, $\mathbf{b}$, can be defined in cartesian coordinates as

$$\mathbf{b} = \begin{bmatrix} b_x \\ b_{\dot{x}} \\ b_y \\ b_{\dot{y}} \\ {b_{tx}}^1 \end{bmatrix}$$

and stance dynamics in cartesian coordinates is

$$\dot{\mathbf{b}} = \begin{bmatrix} \dot{b}_x \\ \dot{b}_{\dot{x}} \\ \dot{b}_y \\ \dot{b}_{\dot{y}} \\ \dot{b}_{tx} \end{bmatrix} = \begin{bmatrix} b_{\dot{x}} \\ \frac{-F_s(q_r, q_{\dot{r}})\sin(q_\theta)}{m} \\ b_{\dot{y}} \\ \frac{F_s(q_r, q_{\dot{r}})\cos(q_\theta)}{m} - g_s \\ 0 \end{bmatrix}$$

$$= \begin{bmatrix} b_{\dot{x}} \\ \frac{-F_s(\sqrt{(b_x - b_{tx})^2 + (b_y - F_g(b_{tx}))^2}, \frac{(b_x - b_{tx})b_{\dot{x}} + (b_y - F_g(b_{tx}))b_{\dot{y}}}{\sqrt{(b_x - b_{tx})^2 + (b_y - F_g(b_{tx}))^2}})\sin(\arctan(\frac{b_y - F_g(b_{tx})}{b_x - b_{tx}}))}{m} \\ b_{\dot{y}} \\ \frac{F_s(\sqrt{(b_x - b_{tx})^2 + (b_y - F_g(b_{tx}))^2}, \frac{(b_x - b_{tx})b_{\dot{x}} + (b_y - F_g(b_{tx}))b_{\dot{y}}}{\sqrt{(b_x - b_{tx})^2 + (b_y - F_g(b_{tx}))^2}})\cos(\arctan(\frac{b_y - F_g(b_{tx})}{b_x - b_{tx}}))}{m} - g_s \\ 0 \end{bmatrix}$$

For simplicity, if we assume flat ground with zero height (i.e. $F_g(x) = 0 \ \forall x$) and the toe of the leg is located at zero ($b_{tx} = 0$), then the stance dynamic in cartesian coordinates becomes

$$\dot{\mathbf{b}} = \begin{bmatrix} b_{\dot{x}} \\ \frac{-F_s(\sqrt{{b_x}^2 + {b_y}^2}, \frac{b_x b_{\dot{x}} + b_y b_{\dot{y}}}{\sqrt{{b_x}^2 + {b_y}^2}})\sin(\arctan(\frac{b_y}{b_x}))}{m} \\ b_{\dot{y}} \\ \frac{F_s(\sqrt{{b_x}^2 + {b_y}^2}, \frac{b_x b_{\dot{x}} + b_y b_{\dot{y}}}{\sqrt{{b_x}^2 + {b_y}^2}})\cos(\arctan(\frac{b_y}{b_x}))}{m} - g_s \\ 0 \end{bmatrix}$$

where $F_s(q_r, q_{\dot{r}})$ is the same as previously defined.

Stance dynamics has several nonintegrable terms due to gravity [4], [12]. Therefore, there is not an exact analytical solution for stance map. There exists several studies on approximate solution of SLIP stance dynamics. In this report, only two of them are considered ([10] and [3]) and a new improvement tool with gravity effect correction is introduced to improve the mapping performance.

2.2.2 Flight Dynamics

As previously stated, flight dynamics of the SLIP is ballistic flow which has a well known analytically solved dynamics. For simplicity, the most suitable coordinate system is cartesian coordinates to analyze the flight dynamics. The state vector, $\mathbf{b}$ can be defined in cartesian coordinates as

$$\mathbf{b} = \begin{bmatrix} b_x \\ b_{\dot{x}} \\ b_y \\ b_{\dot{y}} \\ b_{tx} \end{bmatrix}$$

and the flight dynamics is

$$\dot{\mathbf{b}} = \begin{bmatrix} \dot{b}_x \\ \dot{b}_{\dot{x}} \\ \dot{b}_y \\ \dot{b}_{\dot{y}} \\ \dot{b}_{tx} \end{bmatrix} = \begin{bmatrix} b_{\dot{x}} \\ 0 \\ b_{\dot{y}} \\ -g_f \\ b_{\dot{x}} \end{bmatrix}$$

Coordinate transfer maps can be written to transfer cartesian state vectors to polar state vectors to use both dynamics relations.

The fifth state variable, b_{tx} is only defined for multi-stride locomotion. For single stride locomotion it is not necessary and can be assumed zero. As a side note, it is constant during the stance phase and has the same dynamic equation with body position state, b_x. It is only updated independently from its dynamics when apex event occurs and it is updated with the new touchdown angle.

3 Previous Studies on Approximate Stance Map

Approximate stance map is required for stability analysis of locomotion, control algorithm design and motion planning of the SLIP and SLIP like platforms. Before usage of approximate map for stance phase, several controllers are designed based on the captured data from running video of a designed legged runner or animal, or numerically solved discrete locomotion configurations. For example, in [2], real time deadbeat controller was designed by interpolating the previously solved locomotions, it was an expensive way of designing control law for monoped runner. After stance map approximation studies, several controllers, especially deadbeat controllers, are designed based on the approximate stance maps as in [6], [8] and [11] which are applicable for real time locomotion control and inexpensive compared to [2].

The general idea behind the approximate stance map is the estimating the next apex state from the current apex state with a chosen control set (touchdown angle and leg compliance control).Also, bottom to apex or apex to bottom maps can be necessary for other purpose, e.g. stance map for variable stiffness. Figure 3 represents these maps for a symmetric gait.

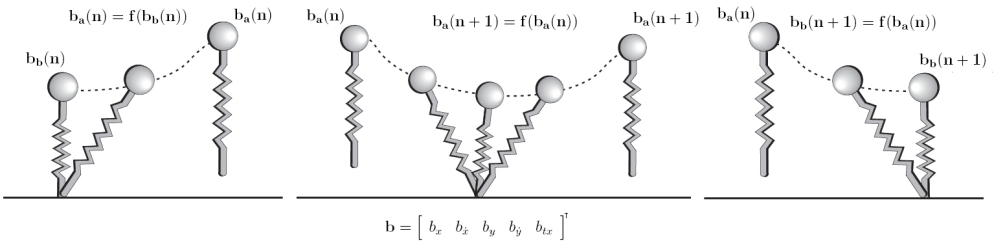

Figure 3: Left: Bottom to Apex Map. Middle: Apex Return Map. Right: Apex to Bottom Map. This figure is taken from [11].

In this section, two previous studies on approximate stance map ([3] and [10]) are examined and their solution approaches are summarized with the notation used in this report. At the end of this section, the proposed gravity effect correction methods are introduced and the necessity of the proposed method is given. Let us begin with the approximate stance map solution proposed by Geyer et al.

3.1 Simple Approximate Stance Map by Geyer et al.

The stance phase dynamics has nonintegrable terms, and to find an analytical solution for stance equations Geyer et al. have used several approximations to have an integrable approximate dynamics for stance phase. The Lagrangian equation during ground contact in polar coordinates (q_r, q_θ) is given by (see Figure 1 and Table 1 for notation)

$$L = \frac{m}{2}(\dot{q_r}^2 + {q_r}^2\dot{q_\theta}^2) - \frac{k}{2}(l_0 - q_r)^2 - mg_s q_r \cos(q_\theta) \tag{1}$$

the equation of motion for the center of mass can be derived from Lagrange function (1) as

$$\begin{aligned}
0 &= \frac{d}{dt}(\frac{dL}{d\dot{q_j}}) - \frac{dL}{dq_j} \\
0 &= \frac{d}{dt}(\frac{dL}{d\dot{q_r}}) - \frac{dL}{dq_r} \\
0 &= \frac{d}{dt}(\frac{dL}{d\dot{q_\theta}}) - \frac{dL}{dq_\theta} \\
m\ddot{q_r} &= mq_r\dot{q_\theta}^2 + k(l_0 - q_r) - mg_s\cos(q_\theta) && (2)\\
0 &= \frac{d}{dt}(m{q_r}^2\dot{q_\theta}) + mg_s q_r \sin q_\theta && (3)
\end{aligned}$$

Since (2) and (3) are coupled nonlinear differential equation and a closed form solution with known basic functions may not be found easily, several approximations are necessary to find an approximate solution.

Assumption 1 *To get rid of some of nonlinear terms, sufficiently small sweep angle, Δq_θ, around zero radian is assumed, in other wolds* $\cos(q_\theta) \approx 1$ *and* $\sin(q_\theta) \approx 0$.

So (2) and (3) become

$$\begin{aligned}
m\ddot{q_r} &= mq_r\dot{q_\theta}^2 + k(l_0 - q_r) - mg_s && (4)\\
\frac{d}{dt}(m{q_r}^2\dot{q_\theta}) &= 0 && (5)
\end{aligned}$$

By this assumption, the motion equation is transformed into integrable dynamics while the total energy, E, and angular momentum, $p_\theta = m{q_r}^2\dot{q_\theta}$, is conserved.

Remark 1 *As a result of assumption 1, it seems that angular momentum is also conserved during stance phase. However, angular momentum is not really conserved due to gravity when there is a ground contact. Therefore, conservation of angular momentum is a result of first assumption.*

From (5) the leg angle, $q_\theta(t)$, can be solved by using the solution of leg length, $q_r(t)$, since $\dot{q_\theta} = \frac{p_\theta}{m{q_r}^2}$. Thus,to find approximate apex return map solution of leg length , $q_r(t)$, is the first crucial requirement.

Since angular momentum, p_θ, and total mechanical energy, E, is conserved, the energy relation can be written as (note that $\cos(q_\theta) \approx 1$ by Assumption 1)

$$E = \frac{m}{2}{\dot{q_r}}^2 + \frac{{p_\theta}^2}{2m{q_r}^2} + \frac{k}{2}(l_0 - q_r)^2 + mg_s q_r. \tag{6}$$

Let us define new parameters

$$\rho = \frac{q_r - l_0}{l_0} \leq 0,\ \epsilon = \frac{2E}{m{l_0}^2},\ \omega = \frac{p_\theta}{m{l_0}^2} \text{ and } \omega_0 = \sqrt{\frac{k}{m}} \tag{7}$$

and substitute them into (6)

$$\epsilon = \dot{\rho}^2 + \frac{\omega^2}{(1+\rho)^2} + {\omega_0}^2\rho^2 + \frac{2g_s}{l_0}(1+\rho) \tag{8}$$

Assumption 2 *ρ represents the relative spring amplitude which gives information about the percentage compression of the spring. To find an analytical solution, it is assumed that spring is allowed to perform small compressions. Therefore, $|\rho| << 1$ and $\frac{1}{(1+\rho)^2}$ can be approximated by Taylor series expansion around zero as given below.*

$$\left.\frac{1}{(1+\rho)^2}\right|_{\rho=0} = 1 - 2\rho + 3\rho^2 - O(\rho^3)$$

Using the result of assumption 2 and Eq.(8), an integrable equation can be written as

$$t = \int \frac{d\rho}{\sqrt{\lambda\rho^2 + \mu\rho + \nu}} \tag{9}$$

where

$$\lambda = -(3\omega^2 + {\omega_0}^2),\ \mu = 2(\omega^2 - gs/l_0) \text{ and } \nu = (\epsilon - \omega^2 - 2g_s/l_0)$$

The solution of the integral in (9) is as below if λ is negative and discriminant of the polynomial $\lambda\rho^2 + \mu\rho + \nu$ (i.e. $\mu^2 - 4\lambda\nu$) is positive. From the definition of λ, it is obvious that it is negative. The second condition is satisfied if ν is positive and it can be checked at the instance of touchdown.

$$\int \frac{d\rho}{\sqrt{\lambda\rho^2 + \mu\rho + \nu}} = -\frac{1}{\sqrt{-\lambda}} \arcsin(\frac{2\lambda\rho + \mu}{\sqrt{\mu^2 - 4\lambda\nu}}) \tag{10}$$

The general radial motion, $q_r(t)$, can be solved as

$$q_r(t) = l_0(1 + a + b\sin(\hat{\omega}_0 t)) \tag{11}$$

where

$$\begin{aligned}
\hat{\omega}_0 &= \sqrt{{\omega_0}^2 + 3\omega^2}, \\
a &= \frac{\omega^2 - g_s/l_0}{{\omega_0}^2 + 3\omega^2} = \frac{\omega^2 - g_s/l_0}{\hat{\omega}_0^2}, \\
b &= \frac{\sqrt{(\omega^2 - g_s/l_0)^2 + ({\omega_0}^2 + 3\omega^2)(\epsilon - \omega^2 - 2g_s/l_0)}}{{\omega_0}^2 + 3\omega^2} \\
&= \sqrt{a^2 + \frac{\epsilon - \omega^2 - 2g_s/l_0}{\hat{\omega}_0^2}}.
\end{aligned}$$

Figure 4 shows one period of the general solution of the leg length during contact phase. As seen from the figure, it is a sinusoidal motion with amplitude $l_0 b$, frequency $\hat{\omega}_0$ and offset $l_0(1 + a)$. Since it is a solution for stance phase, the part of solution where $q_r(t) \leq l_0$ is fulfilled is only valuable. Also, Δl_{max} represents the maximum spring compression and it is the difference between $l_0 b$ and $l_0 a$ ($\Delta l_{max} = l_0 b - l_0 a$). From assumption 3 $|\rho| \ll 1$ and $|\rho| = \frac{\Delta l_{max}}{l_0} = b - a \Rightarrow b - a \ll 1$.

(11) can be used to determine the critical times such as touchdown, bottom and liftoff times. The general formulation of these instances can be done as

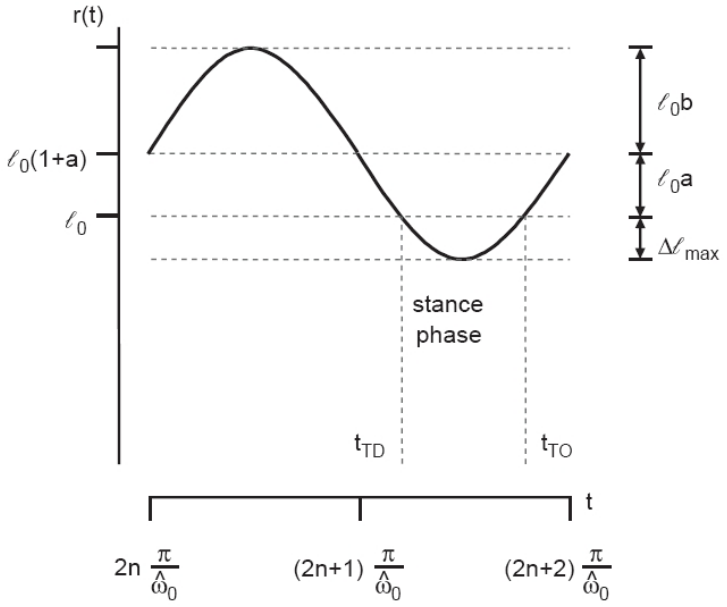

Figure 4: General solution for the leg length, $q_r(t)$ for stance phase. The sinusoidal solution has amplitude $l_0 b$ and frequency $\hat{\omega_0}$ with offset $l_0(1+a)$. Since the solution is only suitable for stance phase, the portion where $q_r \leq l_0$ is significant. a can also be negative in which case l_0 will be above $l_0(1+a)$. Δl_{max} represents the maximum leg compression. This figure is taken from [3].

$$t_{td} = \frac{1}{\hat{\omega}_0}\left\{(2n+\frac{3}{2})\pi - \left[\frac{\pi}{2} + \arcsin(\frac{q_{rtd}/l_0 - 1 - a}{b})\right]\right\} \quad (12)$$

$$t_b = \frac{1}{\hat{\omega}_0}\left\{\left(2n+\frac{3}{2}\right)\pi\right\} \quad (13)$$

$$t_{lo} = \frac{1}{\hat{\omega}_0}\left\{(2n+\frac{3}{2})\pi + \left[\frac{\pi}{2} + \arcsin(\frac{q_{rlo}/l_0 - 1 - a}{b})\right]\right\} \quad (14)$$

where $n \in \mathbf{N}$

(12) and (14) can be simplified for a special case when the liftoff , q_{rlo}, and touchdown, q_{rtd}, leg lengths are equal to rest leg length,l_0

$$t_{td} = \frac{1}{\hat{\omega}_0}\left\{(2n+\frac{3}{2})\pi - \left[\frac{\pi}{2} + \arcsin(-\frac{a}{b})\right]\right\} \quad (15)$$

$$t_{lo} = \frac{1}{\hat{\omega}_0}\left\{(2n+\frac{3}{2})\pi + \left[\frac{\pi}{2} + \arcsin(-\frac{a}{b})\right]\right\} \quad (16)$$

As previously stated, the angular motion of the SLIP can be found from radial motion since the angular momentum is conserved during stance phase (Remark 1). The relation between angular and radial motion is $\dot{q}_\theta = \frac{p_\theta}{m{q_r}^2}$ and by using the previously defined parameters ρ and ω , the angular velocity can be written as

$$\dot{q}_\theta = \frac{\omega}{(1+\rho)^2} \quad (17)$$

The term $\frac{1}{(1+\rho)^2}$ can be linearly approximated by Taylor series expansion as previously done. So, (17) becomes $\dot{q}_\theta = \omega(1-2\rho)$. If we use the definition of ρ, angular motion equation is found as ($\rho = \frac{q_r - l_0}{l_0} = a + b\sin(\hat{\omega}_0 t)$)

$$q_\theta(t) = q_{\theta td} + \int_{t_{td}}^{t} \omega[(1-2a) - 2b\sin(\hat{\omega}_0 t)]dt, \quad (18)$$

$$q_\theta(t) = q_{\theta td} + \omega(1-2a)(t-t_{td}) + \frac{2b\omega}{\hat{\omega}_0}[cos(\hat{\omega}_0 t) - cos(\hat{\omega}_0 t_{td})] \quad (19)$$

where $t_{td} \leq t \leq t_{lo}$ (note that t_{td} and t_{lo} are calculated as in (12)) and (14). Moreover, the stance time, t_s, can be calculated easily as

$$t_s = t_{lo} - t_{td} = [\pi + 2\arcsin(-a/b)]/\hat{\omega}_0 \tag{20}$$

Also if the touchdown instance is scaled to t=0, the leg length and leg angle equations take the form as below while the stance time remains the same as in (20)

$$\begin{aligned} q_r(t) &= l_0 + l_0[a(1-\cos(\hat{\omega}_0 t)) - \sqrt{b^2-a^2}\sin(\hat{\omega}_0 t)] && (21)\\ q_\theta(t) &= q_{\theta td} + (1-2a)\omega t + \frac{2\omega}{\hat{\omega}_0}[a\sin(\hat{\omega}_0 t) + \sqrt{b^2-a^2}(1-cos(\hat{\omega}_0 t))] && (22) \end{aligned}$$

If the predefined parameters a, b, ϵ, ω and ω_0 are replaced by the touchdown states and system parameters and touchdown time instance is selected as zero, the radial and angular motion equation is given by

$$\begin{aligned} q_r(t) &= l_0 - \frac{|q_{\dot{r}td}|}{\hat{\omega}_0}\sin(\hat{\omega}_0 t) + \frac{{q_{\dot{\theta}td}}^2 l_0 - g_s}{\hat{\omega}_0^2}(1-cos(\hat{\omega}_0 t)), && (23)\\ q_\theta(t) &= q_{\theta td} + (1 - 2\frac{{q_{\dot{\theta}td}}^2 - g_s/l_0}{\hat{\omega}_0^2})q_{\dot{\theta}_{td}} t \\ &\quad + \frac{2q_{\dot{\theta}_{td}}}{\hat{\omega}_0}[\frac{{q_{\dot{\theta}td}}^2 - g_s/l_0}{\hat{\omega}_0^2}\sin(\hat{\omega}_0 t) + \frac{|q_{\dot{r}_{td}}|}{\hat{\omega}_0 l_0}(1-cos(\hat{\omega}_0 t))] && (24) \end{aligned}$$

where the oscillation frequency is calculated by $\hat{\omega}_0 = \sqrt{k/m + 3{q_{\dot{\theta}_{td}}}^2}$ and the stance time , t_s and bottom time, t_b, is given by

$$\begin{aligned} t_s &= \frac{1}{\hat{\omega}_0}\left[\pi + 2\arctan(\frac{g_s - l_0{q_{\dot{\theta}_{td}}}^2}{|q_{\dot{r}_{td}}|\hat{\omega}_0})\right] && (25)\\ t_b &= \frac{1}{\hat{\omega}_0}\arctan\left(\frac{|q_{\dot{r}_{td}}|\hat{\omega}_0}{q_{\dot{\theta}_{td}}^2 l_0 - g_s}\right) && (26) \end{aligned}$$

3.2 Approximate Iterative Stance Map by Schwind and Koditschek

The SLIP template has nonintegrable stance dynamics and finding an approximate analytical solution requires several assumptions. In [3], there are some assumptions that limit motion of SLIP with small swept angle and spring compression, and by this limitations and appropriate assumptions the stance dynamics takes an integrable

form. Since there are limitations on locomotion, the performance of the approximation worsen outside the limited motions. Schwind and Koditscheck have proposed another approximation for stance map such that the nonintegrable dynamics can be solved by iterative application of mean value theorem for integral operator. Also, they have showed that this iteration method converges to the exact solution if the method is applied sufficiently many times. Note that their approximation is not whole apex return map, only bottom to apex map is given (see Figure 3).

The stance dynamics for the decompression phase can be written by Hamiltonian mechanics as

$$H = \frac{1}{2m}\left(p_r^2 + \frac{p_\theta^2}{q_r^2}\right) + \frac{1}{2}k_d(l_0 - q_r)^2 + mg_s q_r \cos(q_\theta) \tag{27}$$

and

$$\dot{p}_j = -\frac{dH}{dq_j}\ ,\ \dot{q}_j = \frac{dH}{dp} \tag{28}$$

so the Hamiltonian vector field is given by

$$\mathbf{X_H} = \begin{bmatrix} \dot{q}_r \\ \dot{q}_\theta \\ \dot{p}_r \\ \dot{p}_\theta \end{bmatrix} = \begin{bmatrix} \frac{p_r}{m} \\ \frac{p_\theta}{mq_r^2} \\ \frac{p_\theta^2}{mq_r^3} + k_d(l_0 - q_r) - mg_s\cos(q_\theta) \\ mg_s q_r sin(q_\theta) \end{bmatrix} \tag{29}$$

Using the Harmitonian vector and conservation of energy (the SLIP template does not contain any lossy parameter), the relation between the states can be written as

$$\frac{dt_s}{dq_r}(q_r, q_\theta, p_\theta) = \frac{m}{p_r(q_r, q_\theta, p_\theta)}, \tag{30}$$

$$\frac{dq_\theta}{dq_r}(q_r, q_\theta, p_\theta) = \frac{p_\theta}{q_r^2 p_r(q_r, q_\theta, p_\theta)}, \tag{31}$$

$$\frac{dp_\theta}{dq_r}(q_r, q_\theta, p_\theta) = \frac{m^2 g_s q_r sin(q_\theta)}{p_r(q_r, q_\theta, p_\theta)}, \tag{32}$$

$$\begin{aligned} p_r(q_r, q_\theta, p_\theta, E) &= H^{-1}(q_r, q_\theta, p_\theta, E) \\ &= \sqrt{2m\left(E - \frac{1}{2}k_d(l_0 - q_r)^2 - mg_s q_r\cos(q_\theta)\right) - \frac{p_\theta^2}{q_r^2}} \end{aligned} \tag{33}$$

where E represents the total mechanical energy which is constant,
$H(q_r, q_\theta, p_r, p_\theta) = E$.

Since there is an implicit function for radial momentum, p_r, if the other two state, q_θ and p_θ, are solved then p_r can be calculated by Eq.(33).

However, (30), (31) and (32) are nonlinear coupled differential equations.The exact analytical solution is unknown but by mean value theorem an iterative solution procedure can be driven. In fact, Schwind and Koditschek in [9] have shown the following results:

Theorem 1 *Suppose the function f is continuous on (a,b] and g is integrable on (a,b) with g(t)≥ 0 ∀ t ∈ (a,b). Let x ∈ (a,b]. If both*

$$\lim_{t\to a} \frac{f(t) - K}{(t-a)^r} \quad \lim_{t\to a} \frac{g(t)}{(t-a)^s}$$

exist and are nonzero for some constant K, some nonzero r, and some s > -1 with r+s > -1, then

1. *there exists a $\xi_x \in (a, x]$ such that*

$$\int_a^x f(t)g(t)dt = f(\xi_x) \int_a^x g(t)dt \tag{34}$$

2. *for any such choice of ξ_x*

$$\lim_{x\to a} \frac{\xi_x - a}{x - a} = \left(\frac{s+1}{r+s+1}\right)^{\frac{1}{r}} \tag{35}$$

For the calculation of ξ_x a practical observation is presented in [9].

Observation 1 *If, motivated by (35), ξ_x is approximated by*

$$\hat{\xi}_x = a + \left(\frac{s+1}{r+s+1}\right)^{\frac{1}{r}} (x-a) \text{ for } x \text{ nera } a, \tag{36}$$

and replace ξ_x by $\hat{\xi}_x$ in Eq.(34), an approximation is obtained for the integral as

$$\int_a^x f(t)g(t)dt \approx f(\hat{\xi}_x) \int_a^x g(t)dt \text{ for } x \text{ near } a. \tag{37}$$

Using Theorem 1 and Observation 1 and under reasonable assumptions ξ_x is found as in [10, Appendix A] for the following integrals.

$$\int_{q_{r_b}}^{q_r} \frac{1}{H^{-1}(\sigma, q_\theta, p_\theta, E)} d\sigma \approx \frac{1}{H^{-1}(\hat{\xi}_x, \hat{q}_\theta(\hat{\xi}_x), \hat{p}_\theta(\hat{\xi}_x), E)}(q_r - q_{r_b}) \tag{38}$$

$$\int_{q_{r_b}}^{q_r} \frac{1}{\sigma^2 H^{-1}(\sigma, q_\theta, p_\theta, E)} d\sigma \approx \frac{1}{\hat{\xi}_x^2 H^{-1}(\hat{\xi}_x, \hat{q}_\theta(\hat{\xi}_x), \hat{p}_\theta(\hat{\xi}_x), E)}(q_r - q_{r_b}) \tag{39}$$

$$\int_{q_{r_b}}^{q_r} \frac{\sigma}{H^{-1}(\sigma, q_\theta, p_\theta, E)} d\sigma \approx \frac{\hat{\xi}_x}{H^{-1}(\hat{\xi}_x, \hat{q}_\theta(\hat{\xi}_x), \hat{p}_\theta(\hat{\xi}_x), E)}(q_r - q_{r_b}) \tag{40}$$

where $\hat{\xi}_r$ is found for all of the integrals the same as

$$\hat{\xi}_x = \frac{3}{4} q_{r_b} + \frac{1}{4} q_r \tag{41}$$

Thus, nonlinear coupled differential equations (30),(31) and (32) can be solved iteratively as

$$\hat{t}_{s_{(n+1)}}(q_r) = t_b + \frac{m}{H^{-1}(\hat{\xi}_r, \hat{q}_{\theta_n}(\hat{\xi}_r), \hat{p}_{\theta_n}(\hat{\xi}_r), E)}(q_r - q_{r_b}) \tag{42}$$

$$\hat{q}_{\theta_{(n+1)}}(q_r) = q_{\theta_b} + \frac{\hat{p}_{\theta_n}(\hat{\xi}_r)}{\hat{\xi}_r^2 H^{-1}(\hat{\xi}_r, \hat{q}_{\theta_n}(\hat{\xi}_r), \hat{p}_{\theta_n}(\hat{\xi}_r), E)}(q_r - q_{r_b}) \tag{43}$$

$$\hat{p}_{\theta_{(n+1)}}(q_r) = p_{\theta_b} + \frac{m^2 g_s \hat{\xi}_r \sin(\hat{q}_{\theta_n}(\hat{\xi}_r))}{H^{-1}(\hat{\xi}_r, \hat{q}_{\theta_n}(\hat{\xi}_r), \hat{p}_{\theta_n}(\hat{\xi}_r), E)}(q_r - q_{r_b}) \tag{44}$$

$$\hat{p}_{r_{(n+1)}}(q_r) = \sqrt{2m\left(E - \frac{1}{2}k_d(l_0 - \hat{\xi}_r)^2 - m g_s \hat{\xi}_r \cos(\hat{q}_{\theta_{(n+1)}}(\hat{\xi}_r))\right) - \frac{\hat{p}^2_{\theta_{(n+1)}}(\hat{\xi}_r)}{\hat{\xi}_r^2}} \tag{45}$$

where n is the iteration number.

The zeroth iteration can be any approximate analytical solution for contact phase. In [10] three different initial approximate solutions are used and [3] may be a good initial iteration for this iterative approximation.

4 Stance Map with Gravity Correction

In section 3, the previous studies [3] and [10] on approximate stance map are given and both of the studies are considered to symmetric strides.In [3], Assumption 1 (small sweep angle around zero) shows that symmetric gaits are considered during derivations since symmetric locomotions always have sweep angles around zero.Similarly, in [10] the initial configuration of the locomotion is started from bottom state with verticular leg alignment and vertical leg alignment at bottom state is only realized during symmetric gaits.

However, humans, animals and legged robots sometimes need to use nonsymmetric gaits to slow down, speed up, stop or change direction of motion in sagittal plane. Especially, if one performs a motion planning algorithm for SLIP like systems, well performing controllers for nonsymmetric gaits are needed. One of the way of designing high performance controllers is usage of reliable stance maps for nonsymmetric locomotions.

In this section, we propose several methods to have more reliable apex return map for nonsymmetric gaits, our methods are built on the results on [3]. During stance map derivation in [3], conservation of angular momentum is a consequence of Assumption 1. In fact, angular momentum is not conserved due to gravity for both symmetric and nonsymmetric gaits when there is a ground contact.There is a special case for symmetric gait states as

$$\begin{aligned} q_{r_{lo}} &= q_{r_{td}} \\ q_{\dot{r}_{lo}} &= -q_{\dot{r}_{td}} \\ q_{\theta_{lo}} &= q_{\theta_{td}} - \Delta q_{\theta} \\ q_{\dot{\theta}_{lo}} &= q_{\dot{\theta}_{td}} \end{aligned}$$

and the angular momentum at liftoff is the same as the angular momentum at touchdown, so angular momentum is *"conserved"* for mapping from touchdown state to liftoff state which means total effect of gravity on angular momentum from touchdown to liftoff is zero for symmetric strides. Thus, conservation of angular momentum can be a reasonable assumption for symmetric gaits. On the other side, there is a total nonzero effect of gravity on angular momentum for nonsymmetric locomotion for mapping from touchdown to takeoff. In the following subsections, we propose several

methods to take into account this gravity effect with virtual gravity effect on angular momentum. When we only consider the stance phase (see Figure 5), the general effect of the gravity on angular moment can be modeled as

$$\tau(t) = \frac{dP(t)}{dt} \quad \Leftrightarrow \quad P(t) = P_{t_0} + \int_{t_0}^{t} \tau(\zeta) d\zeta \tag{46}$$

$$\tau(t) \quad = \quad m g_s q_r(t) \sin(q_\theta(t)) \tag{47}$$

$$P(t) = P_{t_0} + \int_{t_0}^{t} \tau(\zeta) d\zeta \quad \approx \quad P_{t_0} + (t - t_0) \left(\frac{1}{n} \sum_{k=1}^{n} m g q_r(n) \sin(q_\theta(n)) \right) \tag{48}$$

where n is number of samples during stance locomotion.

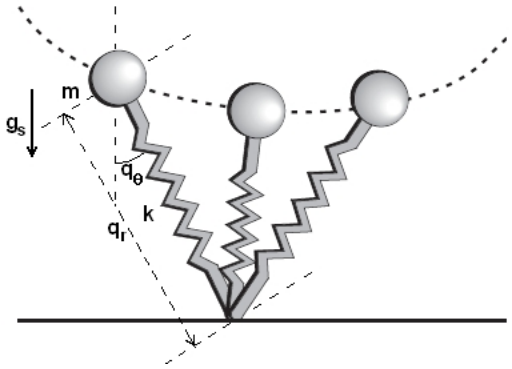

Figure 5: SLIP Stance Phase. This figure is taken from [11].

4.1 Gravity Correction Type 0

Gravity Correction Type 0 is a method such that the total gravity effect on angular momentum from touchdown to liftoff is modeled with a constant virtual effect. The virtual effect is calculated by assuming that leg length is constant and equal to rest leg length during stance phase, $q_r(t) \approx l_0$. Also, the samples of the motion are assumed to be taken at touchdown and liftoff instances. Using (48), the virtual gravity effect resolves to

$$P_c(t) = \frac{t_s m g_s l_0}{2} \left(\sin(q_{\theta_{td}}) + \sin(q_{\theta_{lo}}) \right) \tag{49}$$

parameters $t_{td}, t_{lo}, t_s = t_{lo} - t_{td}, q_{\theta_{td}}$ and $q_{\theta_{td}}$ can be calculated by using any related formula in section 3.1.

We propose to use the virtual effect, $P_c(t)$ given as in (49), as a correction term added to original angular momentum which is assumed to be conserved during for-

mulation in [3]. Therefore, we have only modified the parameter p_θ and rest of the formulation stays the same.

$$\hat{p}_\theta(t) = p_\theta + P_c(t) \tag{50}$$

Moreover, bottom instance can be taken into account as a sampling time since it is also a critical instance of locomotion. Thus the formula for virtual gravity effect changes slightly and usage of the correction term is the same as above.

$$P_c(t) = \frac{t_s m g_s l_0}{3} \left(\sin(q_{\theta_{td}}) + \sin(q_{\theta_b}) + \sin(q_{\theta_{lo}})\right) \tag{51}$$

similarly, parameters $t_{td}, t_{lo}, t_b, t_s = t_{lo} - t_{td}, q_{\theta_{td}}, q_{\theta_b}$ and $q_{\theta_{td}}$ can be calculated by using any related formula in section 3.1.

4.2 Gravity Correction Type 1

Gravity Correction Type 1 is another method such that the total gravity effect on angular momentum from touchdown to liftoff is modeled with a constant virtual effect. The virtual effect is calculated by assuming that leg length is constant and equal to average of rest leg length and bottom leg length during stance phase, $q_r(t) \approx \frac{l_0 + q_{r_b}}{2}$. Also, the samples of the motion are assumed to be taken at touchdown and liftoff instances. Using (48), the virtual gravity effect resolves to

$$P_c(t) = t_s m g_s \frac{l_0 + q_{r_b}}{4} \left(\sin(q_{\theta_{td}}) + \sin(q_{\theta_{lo}})\right) \tag{52}$$

parameters $t_{td}, t_{lo}, t_b, t_s = t_{lo} - t_{td}, q_{r_b}, q_{\theta_{td}}$ and $q_{\theta_{td}}$ can be calculated by using any related formula in section 3.1.

We propose to use the virtual effect, $P_c(t)$ given as in (52), as a correction term added to original angular momentum which is assumed to be conserved during formulation in [3]. Therefore, we have only modified the parameter p_θ and rest of the formulation stays the same.

$$\hat{p}_\theta(t) = p_\theta + P_c(t) \tag{53}$$

Moreover, bottom instance can be taken into account as a sampling time since it is also a critical instance of locomotion. Thus the formula for virtual gravity effect

changes slightly and usage of the correction term is the same as above.

$$P_c(t) = t_s m g_s \frac{l_0 + q_{r_b}}{6} \left(\sin(q_{\theta_{td}}) + \sin(q_{\theta_b}) + \sin(q_{\theta_{lo}})\right) \tag{54}$$

similarly, parameters $t_{td}, t_{lo}, t_b, t_s = t_{lo} - t_{td}, q_{r_b}, q_{\theta_{td}}, q_{\theta_b}$ and $q_{\theta_{td}}$ can be calculated by using any related formula in section 3.1.

4.3 Gravity Correction Type 2

Gravity Correction Type 2 is third method such that the total gravity effect on angular momentum from touchdown to liftoff is modeled with a constant virtual effect. The virtual effect is calculated by assuming that leg length is constant and equal to average leg length during stance phase, $q_r(t) \approx q_{r_{av}}$.

Using (11) average leg length is derived as

$$\begin{aligned} q_{r_{av}} &= \frac{1}{t_{lo} - t_{td}} \int_{t_{td}}^{t_{lo}} l_0(1 + a + b\sin(\hat{\omega}_0 t))dt & (55)\\ &= l_0(1+a) - \frac{b}{\hat{\omega}_0(t_{lo} - t_{td})}(\cos(\hat{\omega}_0 t_{lo}) - \cos(\hat{\omega}_0 t_{td})) & (56)\\ &= l_0(1+a) - \frac{b}{\hat{\omega}_0 t_s}(\cos(\hat{\omega}_0 t_{lo}) - \cos(\hat{\omega}_0 t_{td})) & (57) \end{aligned}$$

parameters $a, b, \hat{\omega}_0, t_{td}, t_{lo}$ and $t_s = t_{lo} - t_{td}$ can be calculated any related formula in section 3.1.

Using (21) average leg length is given by

$$\begin{aligned} q_{r_{av}} &= \frac{1}{t_s} \int_0^{t_s} \left(l_0 + l_0[a(1 - \cos(\hat{\omega}_0 t)) - \sqrt{b^2 - a^2}\sin(\hat{\omega}_0 t)]\right) dt & (58)\\ &= l_0(1+a) - \frac{l_0}{t_s \hat{\omega}_0}\left[a\sin(\hat{\omega}_0 t_s) + \sqrt{b^2 - a^2}(1 - \cos(\hat{\omega}_0 t_s))\right] & (59) \end{aligned}$$

parameters $a, b, \hat{\omega}_0$ and $t_s = t_{lo} - t_{td}$ can be calculated any related formula in section 3.1.

Using (23) average leg length is resolved to

$$\begin{aligned} q_{r_{av}} &= \frac{1}{t_s} \int_0^{t_s} \left(l_0 - \frac{|q_{\dot{r}td}|}{\hat{\omega}_0}\sin(\hat{\omega}_0 t) + \frac{{q_{\dot{\theta}td}}^2 l_0 - g_s}{\hat{\omega}_0^2}(1 - cos(\hat{\omega}_0 t))\right) dt & (60)\\ &= l_0 + \frac{{q_{\dot{\theta}td}}^2 l_0 - g_s}{\hat{\omega}_0^2} - \frac{|q_{\dot{r}td}|}{\hat{\omega}_0^2 t_s}(1 - \cos(\hat{\omega}_0 t_s)) - \frac{{q_{\dot{\theta}td}}^2 l_0 - g_s}{\hat{\omega}_0^3 t_s}\sin(\hat{\omega}_0 t_s) & (61) \end{aligned}$$

where the oscillation frequency is calculated by $\hat{\omega}_0 = \sqrt{k/m + 3{q_{\dot{\theta}_{td}}}^2}$ and the stance time , t_s is given by (25).

Also, the samples of the motion are assumed to be taken at touchdown and liftoff instances. Using (48), the virtual gravity effect resolves to

$$P_c(t) = \frac{t_s m g_s q_{r_{av}}}{2} \left(\sin(q_{\theta_{td}}) + \sin(q_{\theta_{lo}})\right) \tag{62}$$

parameters $t_{td}, t_{lo}, t_s = t_{lo} - t_{td}, q_{\theta_{td}}$ and $q_{\theta_{td}}$ can be calculated by using any related formula in section 3.1.

We propose to use the virtual effect, $P_c(t)$ given as in (62), as a correction term added to original angular momentum which is assumed to be conserved during formulation in [3]. Therefore, we have only modified the parameter p_θ and rest of the formulation stays the same.

$$\hat{p}_\theta(t) = p_\theta + P_c(t) \tag{63}$$

Moreover, bottom instance can be taken into account as a sampling time since it is also a critical instance of locomotion. Thus the formula for virtual gravity effect changes slightly and usage of the correction term is the same as above.

$$P_c(t) = \frac{t_s m g_s q_{r_{av}}}{3} \left(\sin(q_{\theta_{td}}) + \sin(q_{\theta_b}) + \sin(q_{\theta_{lo}})\right) \tag{64}$$

similarly, parameters $t_{td}, t_{lo}, t_s = t_{lo} - t_{td}, q_{\theta_{td}}, q_{\theta_b}$ and $q_{\theta_{td}}$ can be calculated by using any related formula in section 3.1.

4.4 Gravity Correction Type 3

Gravity correction type 3 is another method such that total gravity effect on angular momentum from any initial stance state to any final stance state is modeled with a constant virtual effect. Gravity correction types 0-2 are proposed especially for apex return map and gravity correction type 0 is a special case of type 3 such that the initial stance state is touchdown state and the final stance state is liftoff state.

Let t_i and t_f be initial and final state times such that $t_{td} \leq t_i < t_f \leq t_{lo}$. Using Eq.(48), the virtual gravity effect resolves to

$$P_c(t) = \frac{(t_f - t_i) m g_s}{2} \left[q_r(t_i) \sin(q_\theta(t_i)) + q_r(t_f) \sin(q_\theta(t_f))\right] \tag{65}$$

where $t_{td}, t_{lo}, q_r(t)$ and $q_\theta(t)$ are defined as in section 3.1.

We propose to use the virtual effect, $P_c(t)$ given as (65) , as a correction term added to original angular momentum which is assumed to be conserved during formulation in [3]. Therefore, we have only modified the parameter p_θ and rest of the formulation stays the same.

$$\hat{p}_\theta(t) = p_\theta + P_c(t) \tag{66}$$

A special case of initial and final state times are touchdown and liftoff times, and also if touchdown and liftoff leg lengths are set to be rest leg length, then correction type 3 is the same as correction type 0.

Moreover, this correction type is valuable for variable stiffness case since the apex return map is derived by dividing the return map into two as apex to bottom and bottom to apex maps. And in this parts of the maps the virtual gravity effect on angular momentum is calculated by touchdown, bottom and liftoff states separately for each parts of the apex return map.

4.5 Gravity Correction Type 4

Gravity correction type 4 is fifth method such that total gravity effect on angular momentum from any initial stance state to any final stance state is modeled with a constant virtual effect by using the average leg length during this period. The virtual effect is calculated by assuming that leg is constant and equal to average leg length, $q_{av}(t_i, t_f)$ during period of motion from initial state to final state. Gravity correction types 0-2 are proposed especially for apex return map and gravity correction type 2 is a special case of type 4 such that the initial stance state is touchdown state and the final stance state is liftoff state.

Let t_i and t_f are initial and final state times such that $t_{td} \leq t_i < t_f \leq t_{lo}$. Using (11) average leg length is derived as

$$\begin{aligned} q_{r_{av}}(t_i, t_f) &= \frac{1}{t_f - t_i} \int_{t_i}^{t_f} l_0(1 + a + b\sin(\hat{\omega}_0 t))dt & (67) \\ &= l_0(1+a) - \frac{b}{\hat{\omega}_0(t_f - t_i)}(\cos(\hat{\omega}_0 t_f) - \cos(\hat{\omega}_0 t_i)) & (68) \\ & & (69) \end{aligned}$$

where a, b and $\hat{\omega}_0$ can be calculated by using any related formula in section 3.1.

Using (21) average leg length is given by (note that $t_{td} = 0$)

$$\begin{aligned} q_{r_{av}}(t_i, t_f) &= \frac{1}{t_f - t_i} \int_{t_i}^{t_f} \left(l_0 + l_0[a(1 - \cos(\hat{\omega}_0 t)) - \sqrt{b^2 - a^2}\sin(\hat{\omega}_0 t)] \right) dt \quad (70) \\ &= l_0(1 + a) - \frac{l_0}{(t_f - t_i)\hat{\omega}_0} [a(\sin(\hat{\omega}_0 t_f) - \sin(\hat{\omega}_0 t_i)) \quad (71) \\ &\quad -\sqrt{b^2 - a^2}(\cos(\hat{\omega}_0 t_f) - \cos(\hat{\omega}_0 t_i))\Big] \quad (72) \end{aligned}$$

parameters a, b and $\hat{\omega}_0$ can be calculated by using any related formula in section 3.1.

Using (23) average leg length is resolved to (note that $t_{td} = 0$)

$$\begin{aligned} q_{r_{av}}(t_i, t_f) &= \frac{1}{t_f - t_i} \int_{t_i}^{t_f} \left(l_0 - \frac{|q_{\dot{r}td}|}{\hat{\omega}_0}\sin(\hat{\omega}_0 t) + \frac{{q_{\dot{\theta}td}}^2 l_0 - g_s}{\hat{\omega}_0^2}(1 - cos(\hat{\omega}_0 t)) \right) dt \quad (73) \\ &= l_0 + \frac{{q_{\dot{\theta}td}}^2 l_0 - g_s}{\hat{\omega}_0^2} + \frac{|q_{\dot{r}td}|}{\hat{\omega}_0^2(t_f - t_i)}[\cos(\hat{\omega}_0 t_f) - \cos(\hat{\omega}_0 t_i)] \quad (74) \\ &\quad -\frac{{q_{\dot{\theta}td}}^2 l_0 - g_s}{\hat{\omega}_0^3(t_f - t_i)}[\sin(\hat{\omega}_0 t_f) - \sin(\hat{\omega}_0 t_i)] \quad (75) \end{aligned}$$

where the oscillation frequency is calculated by $\hat{\omega}_0 = \sqrt{k/m + 3{q_{\dot{\theta}_{td}}}^2}$.

Using Eq.(48), the virtual gravity effect resolves to

$$P_c(t) = \frac{(t_f - t_i) m g_s q_{r_{av}}(t_i, t_f)}{2} \left(\sin(q_\theta(t_i)) + \sin(q_\theta(t_f))\right) \quad (76)$$

where $q_\theta(t)$ is given in section 3.1 for different $q_{r_{av}}(t_i, t_f)$ formulations.

We propose to use the virtual effect, $P_c(t)$ given as in (76), as a correction term added to original angular momentum which is assumed to be conserved during formulation in [3]. Therefore, we have only modified the parameter p_θ and rest of the formulation stays the same.

$$\hat{p}_\theta(t) = p_\theta + P_c(t) \quad (77)$$

A special case of initial and final state times are touchdown and liftoff times,for this special case correction type 4 is the same as correction type 2.

Moreover, this correction type is valuable for variable stiffness case since the apex return map is derived by dividing the return map into two as apex to bottom and bottom to apex maps. And in this parts of the maps the virtual gravity effect on angular momentum is calculated by touchdown, bottom and liftoff states separately for each parts of the apex return map.

4.6 Gravity Correction Type 5

Gravity Correction Type 5 is last method such that the total gravity effect on angular momentum during stance phase is approximated with a time-variant virtual effect.To calculate the virtual gravity effect, leg length and leg angle during stance is approximated by 5 degree polynomial, $q_r(t) \approx q_{r_{av}}$. Using (11) average leg length derived as

5 Approximate Stance Map for Variable Stiffness

There are not too much control parameters for SLIP template since it is the simplest model for legged systems, animals and human. Touchdown leg angle is an indispensable control parameter for stable locomotion. Other control feature is compliance leg parameters to adjust total energy of the model such that characteristic properties of locomotion, apex velocity and height, can be brought to desired levels. In general there are two different approaches to use stiffness property of leg for control of locomotion. First one is that the spring constant is assumed to be constant during stance phase and touchdown and liftoff leg lengths can be controlled to store or release energy from the system.In [1] and [13] similar approach is used on an experimental robotic platform , bow legged hopping robot, and total energy of the robot is controller by compressing stiff leg during flight phase to store energy.Also, in [6] a deadbeat gait controller for a bipedal is designed by adjusting touchdown and liftoff leg lengths. Second approach is controlling spring constants during compression and decompression phases to modify the total system energy. The simulation and experimental studies on this approach have been done by Raibert in [5] and the control of leg spring constant is done by adjusting air pressure in leg piston by a pneumatic actuator during flight phase for compression phase spring constant and at the bottom instance for decompression phase spring constant.

In our studies, we are planning to use variable spring control approach as one of the control strategy with touchdown angle control for motion planning of SLIP in 2D. Therefore, we need approximate stance map for variable stiffness case. In this section, two different approximate stance maps built on [3] and [10] are introduced. The main difference of variable stiffness stance map from the constant stiffness one is two different spring constant can be used for compression and decompression phase. Therefore, apex return map should be divided into two parts, apex to bottom map and bottom to apex map, where different spring constants are employed. The general idea for variable stiffness stance map is represented in Figure 6.

5.1 Simple Approximate Stance Map For Variable Stiffness

In [3] approximate apex return map has been found as a formula of model parameters,touchdown states, total energy and angular momentum while spring constant is not variable during stance phase.Also since SLIP template has not lossy components,

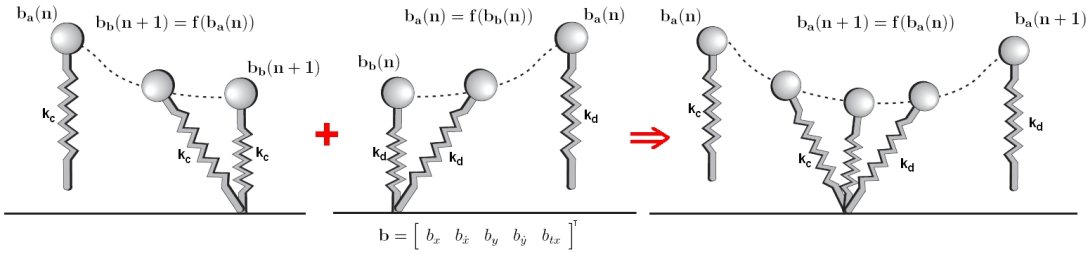

Figure 6: SLIP apex return map for variable stiffness case . Variable stiffness Apex Return Map = Apex to Bottom Map with k_c + Bottom to Apex Map with k_d.

total energy of the system is conserved. However, for variable compliance case, total energy of the model can be modified by controlling the spring constant at bottom instance, so total energy is not constant during stance map and there is a discrete change on total energy at bottom instance. Therefore, apex return map can be obtained by considering apex to bottom map and bottom to apex map separately as in Figure 6.

5.1.1 Apex to Bottom Map

Apex to bottom map can be easily written from results of [3]

$$q_r(t) = l_0(1 + a_{ab} + b_{ab}\sin(\hat{\omega}_{0_{ab}}t)) \tag{78}$$

$$q_\theta(t) = q_{\theta td} + \omega(1 - 2a_{ab})(t - t_{td}) + \frac{2b_{ab}\omega_{ab}}{\hat{\omega}_{0_{ab}}}[cos(\hat{\omega}_{0_{ab}}t) - cos(\hat{\omega}_{0_{ab}}t_{td})] \tag{79}$$

where $t_{td} \leq t \leq t_{b_{ab}}$. t_{td} and $t_{b_{ab}}$ are given by

$$t_{td} = \frac{1}{\hat{\omega}_{0_{ab}}}\left\{(2n + \frac{3}{2})\pi - \left[\frac{\pi}{2} + \arcsin(\frac{q_{r_{td}}/l_0 - 1 - a_{ab}}{b_{ab}})\right]\right\} \tag{80}$$

$$t_{b_{ab}} = \frac{1}{\hat{\omega}_{0_{ab}}}\left\{(2n + \frac{3}{2})\pi\right\} \tag{81}$$

where $n \in \mathbf{N}$ and the parameters $a_{ab}, b_{ab}, \omega_{ab}$ and $\hat{\omega}_{0_{ab}}$ are defined as

$$\epsilon_{ab} = \frac{2E_{ab}}{m{l_0}^2} \tag{82}$$

$$\omega_{ab} = \frac{p_\theta}{m{l_0}^2} \tag{83}$$

$$\omega_{0_{ab}} = \sqrt{\frac{k_c}{m}} \tag{84}$$

$$\hat{\omega}_{0_{ab}} = \sqrt{{\omega_{0_{ab}}}^2 + 3{\omega_{ab}}^2}, \tag{85}$$

$$a_{ab} = \frac{{\omega_{ab}}^2 - g_s/l_0}{{\omega_{0_{ab}}}^2 + 3{\omega_{ab}}^2} = \frac{{\omega_{ab}}^2 - g_s/l_0}{\hat{\omega}_{0_{ab}}^2}, \tag{86}$$

$$b_{ab} = \frac{\sqrt{({\omega_{ab}}^2 - g_s/l_0)^2 + ({\omega_{0_{ab}}}^2 + 3{\omega_{ab}}^2)(\epsilon_{ab} - {\omega_{ab}}^2 - 2g_s/l_0)}}{{\omega_{0_{ab}}}^2 + 3{\omega_{ab}}^2} \tag{87}$$

$$= \sqrt{a_{ab}^2 + \frac{\epsilon_{ab} - {\omega_{ab}}^2 - 2g_s/l_0}{\hat{\omega}_{0_{ab}}^2}}. \tag{88}$$

where E_{ab} is touchdown total energy, which is conserved during compression phase, and p_θ is total angular momentum during stance phase and it is assumed to be conserved during compression phase.

Also (80) can be simplified for a special case when touchdown leg length, $q_{r_{td}}$, is equal to rest leg length, l_0,

$$t_{td} = \frac{1}{\hat{\omega}_{0_{ab}}} \left\{ (2n + \frac{3}{2})\pi - \left[\frac{\pi}{2} + \arcsin(-\frac{a_{ab}}{b_{ab}}) \right] \right\} \tag{89}$$

5.1.2 Bottom to Apex Map

Bottom to apex map has the same form of apex to bottom map solution

$$q_r(t) = l_0(1 + a_{ba} + b_{ba}\sin(\hat{\omega}_{0_{ba}}(t + t_{b_{ba}} - t_{b_{ab}}))) \tag{90}$$

$$q_\theta(t) = q_{\theta b} + \omega(1 - 2a_{ba})(t - t_{b_{ab}}) \tag{91}$$

$$+ \frac{2b_{ba}\omega_{ba}}{\hat{\omega}_{0_{ba}}}[cos(\hat{\omega}_{0_{ba}}(t + t_{b_{ba}} - t_{b_{ab}})) - cos(\hat{\omega}_{0_{ba}} t_{b_{ba}})] \tag{92}$$

where $t_{b_{ab}} \leq t \leq t_{lo}$. $t_{b_{ab}}$ is calculated by Eq.(81) and $t_{b_{ba}}$ and t_{lo} are given by (note that the bottom times may be different due to formulization since spring constants are not the same for compression and decompression phases, therefore there must be time shift for derivations of bottom to apex map)

$$t_{b_{ba}} = \frac{1}{\hat{\omega}_{0_{ba}}} \left\{ (2n + \frac{3}{2})\pi \right\} \tag{93}$$

$$t_{lo} = \frac{1}{\hat{\omega}_{0_{ba}}} \left\{ (2n + \frac{3}{2})\pi + \left[\frac{\pi}{2} + \arcsin(\frac{q_{r_{lo}}/l_0 - 1 - a_{ba}}{b_{ba}}) \right] \right\} + t_{b_{ab}} - t_{b_{ba}} \tag{94}$$

$$\tag{95}$$

(94) can be simplified for a special case when liftoff leg length, $q_{r_{lo}}$, is equal to rest leg length, l_0,

$$t_{l_0} = \frac{1}{\hat{\omega}_{0_{ba}}} \left\{ (2n + \frac{3}{2})\pi + \left[\frac{\pi}{2} + \arcsin(-\frac{a_{ba}}{b_{ba}}) \right] \right\} + t_{b_{ab}} - t_{b_{ba}} \tag{96}$$

where $n \in \mathbf{N}$.

Remark 2 *$p_\theta = m q_r^2 q_{\dot{\theta}}$ is conserved during compression and decompression phases separately. To check if total angular momentum is conserved during all stance phase, the states just before and after bottom instance must be controlled. During bottom instance, we only change the spring constant, so there are discrete jumps on total energy and spring force. Thus, acceleration states may have discrete jumps but velocity and position states are continuous after bottom event. Total angular momentum depends on the position and velocity states, therefore it is continuous and constant during stance phase.*

Remark 3 *At bottom instance, spring constant is changed based on a control algorithm and some amount of energy is stored or released from springy leg. This additional energy is given by*

$$E_{additional} = \frac{1}{2}(k_d - k_c)(l_0 - q_{r_b})^2 \tag{97}$$

where q_{r_b} and t_b can be calculated by (78) and (81).Thus, total energy during decompression phase, E_{ba}, is given by

$$E_{ba} = E_{ab} + E_{additional} = E_{ab} + \frac{1}{2}(k_d - k_c)(l_0 - q_r(t_b))^2 \tag{98}$$

Parameters $a_{ba}, b_{ba}, \omega_{ba}$ and $\hat{\omega}_{0_{ba}}$ are defined for (90)-(96) as

$$\epsilon_{ba} = \frac{2E_{ba}}{m{l_0}^2} \tag{99}$$

$$\omega_{ba} = \frac{p_\theta}{m{l_0}^2} = \omega_{ab} \tag{100}$$

$$\omega_{0_{ba}} = \sqrt{\frac{k_d}{m}} \tag{101}$$

$$\hat{\omega}_{0_{ba}} = \sqrt{{\omega_{0_{ba}}}^2 + 3{\omega_{ba}}^2}, \tag{102}$$

$$a_{ba} = \frac{{\omega_{ba}}^2 - g_s/l_0}{{\omega_{0_{ba}}}^2 + 3{\omega_{ba}}^2} = \frac{{\omega_{ba}}^2 - g_s/l_0}{\hat{\omega}_{0_{ba}}^2}, \tag{103}$$

$$b_{ba} = \frac{\sqrt{({\omega_{ba}}^2 - g_s/l_0)^2 + ({\omega_{0_{ba}}}^2 + 3{\omega_{ba}}^2)(\epsilon_{ba} - {\omega_{ba}}^2 - 2g_s/l_0)}}{{\omega_{0_{ba}}}^2 + 3{\omega_{ba}}^2} \tag{104}$$

$$= \sqrt{a_{ba}^2 + \frac{\epsilon_{ba} - {\omega_{ba}}^2 - 2g_s/l_0}{\hat{\omega}_{0_{ba}}^2}}. \tag{105}$$

Remark 4 *The above formulation of bottom to apex map may cause discontinuities on position and velocity states for whole stance map as in Figure 7. Because parameters of bottom to apex map are solved without considering the continuity of position and velocity parameters.* q_{θ_b} *and* $q_{\dot{r}_b}$ *are continuous due to solution formulation, so we only need to constrain continuity of* $q_r(t)$ *and* $q_{\dot{\theta}}(t)$ *at bottom instance. Note that, the general expression for* $q_r(t)$ *and* $q_{\dot{\theta}}(t)$ *are as*

$$q_r(t) = l_0(1 + a + b\sin(\hat{\omega}_0)t) \tag{106}$$

$$q_{\dot{\theta}}(t) = \omega(1 - 2a - 2b\sin(\hat{\omega}_0)t) \tag{107}$$

continuity constraints (note that $\omega_{ab} = \omega_{ba}$ *)*

$$l_0(1 + a_{ab} + b_{ab}\sin(\hat{\omega}_{0_{ab}} t_{b_{ab}})) = l_0(1 + a_{ba} + b_{ba}\sin(\hat{\omega}_{0_{ba}} t_{b_{ba}})) \tag{108}$$

$$\omega_{ab}(1 - 2a_{ab} - 2b_{ab}\sin(\hat{\omega}_{0_{ab}} t_{b_{ab}})) = \omega_{ba}(1 - 2a_{ba} - 2b_{ba}\sin(\hat{\omega}_{0_{ba}} t_{b_{ba}})) \tag{109}$$

Using (81) and (93), relation between parameters a_{ab}, b_{ab}, a_{ba} *and* b_{ba} *is found as*

$$a_{ab} - b_{ab} = a_{ba} - b_{ba} \tag{110}$$

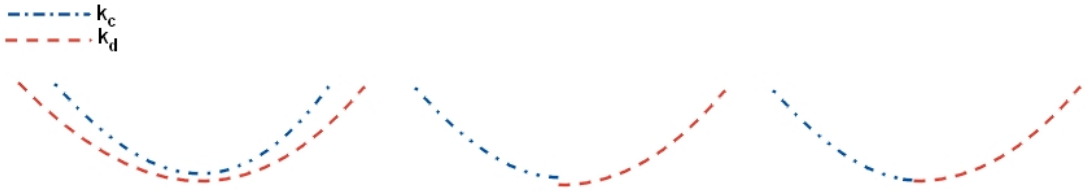

Figure 7: Left:Separate Approximate Stance Map for not variable compliance with spring constants k_c and k_d. Middle: Approximate Stance Map for Variable Stiffness with only parameter updates. A discontinuity is observed on stance map at bottom instance. Right: Approximate Stance Map for variable stiffness with parameter updates and velocity and position state continuity constraints

(110) is the constraint on a_{ba} and b_{ba} for a continuous stance map with variable stiffness. (103) and (104) are unconstraint parametric solutions for a_{ba} and b_{ba}. To prevent discontinuity for stance map,we assume trajectory of decompression phase is invariant under small shift operation, so the offset term of $q_r(t)$ is needed to be reformulated, which means that continuity constraint is used for calculation of a_{ba} and b_{ba} is given by (104).

$$a_{ba} = a_{ab} - b_{ab} + b_{ba} \tag{111}$$

Therefore, the stance map for variable stiffness case is given by

$$q_r(t) = \begin{cases} l_0(1 + a_{ab} + b_{ab}\sin(\hat{\omega}_{0_{ab}}t)), & \text{if } t_{td} \le t \le t_{b_{ab}} \\ l_0(1 + a_{ba} + b_{ba}\sin(\hat{\omega}_{0_{ba}}(t + t_{b_{ba}} - t_{b_{ab}}))), & \text{if } t_{b_{ab}} \le t \le t_{lo} \end{cases} \tag{112}$$

$$q_\theta(t) = \begin{cases} q_{\theta td} + \omega_{ab}(1 - 2a_{ab})(t - t_{td}) \\ \quad + \frac{2b_{ab}\omega_{ab}}{\hat{\omega}_{0_{ab}}}[cos(\hat{\omega}_{0_{ab}}t) - cos(\hat{\omega}_{0_{ab}}t_{td})], \text{ if } t_{td} \le t \le t_{b_{ab}} \\ q_{\theta b} + \omega_{ba}(1 - 2a_{ba})(t - t_{b_{ab}}) \\ \quad + \frac{2b_{ba}\omega_{ba}}{\hat{\omega}_{0_{ba}}}[cos(\hat{\omega}_{0_{ba}}(t + t_{b_{ba}} - t_{b_{ab}})) - cos(\hat{\omega}_{0_{ba}}t_{b_{ba}})], \text{ if } t_{b_{ab}} \le t \le t_{lo} \end{cases} \tag{113}$$

5.2 Iterative Approximate Stance Map For Variable Stiffness

Similarly, using results of [10] and idea of apex return map partitioning into apex to bottom and bottom to apex maps as in Figure 7, an iterative approximate stance

map is derived. In [10] iterative bottom to apex map is already given and in a similar manner apex to bottom iterative approximate map is derived and algorithm for the iterative apex return map for variable stiffness is given. Moreover, a slightly different iterative approximate stance map is derived by varied application of mean value theorem from [10] for both apex to bottom and bottom to apex.

5.2.1 Apex to Bottom Map

SLIP stance dynamics for compression phase can be written by Hamiltonian mechanics as

$$H_{ab} = \frac{1}{2m}\left(p_r^2 + \frac{p_\theta^2}{q_r^2}\right) + \frac{1}{2}k_c(l_0 - q_r)^2 + mg_s q_r \cos(q_\theta) \tag{114}$$

so the Hamiltonian vector field is given by

$$\mathbf{X_{H_{ab}}} = \begin{bmatrix} \dot{q}_r \\ \dot{q}_\theta \\ \dot{p}_r \\ \dot{p}_\theta \end{bmatrix} = \begin{bmatrix} \frac{p_r}{m} \\ \frac{p_\theta}{mq_r^2} \\ \frac{p_\theta^2}{mq_r^3} + k_c(l_0 - q_r) - mg_s\cos(q_\theta) \\ mg_s q_r sin(q_\theta) \end{bmatrix} \tag{115}$$

Using the Hamiltonian vector and conservation of energy (since the SLIP template does not contain any lossy component), the relation between the states can be written as (note that p_r is negative during compression and magnitude is found by Hamiltonian inverse)

$$\begin{aligned}
\frac{dt_s}{dq_r}(q_r, q_\theta, p_\theta) &= \frac{m}{p_r(q_r, q_\theta, p_\theta)}, && (116)\\
\frac{dq_\theta}{dq_r}(q_r, q_\theta, p_\theta) &= \frac{p_\theta}{q_r^2 p_r(q_r, q_\theta, p_\theta)}, && (117)\\
\frac{dp_\theta}{dq_r}(q_r, q_\theta, p_\theta) &= \frac{m^2 g_s q_r sin(q_\theta)}{p_r(q_r, q_\theta, p_\theta)}, && (118)\\
p_r(q_r, q_\theta, p_\theta, E_{ab}) &= -H_{ab}^{-1}(q_r, q_\theta, p_\theta, E_{ab}) \\
&= -\sqrt{2m\left(E_{ab} - \frac{1}{2}k_d(l_0 - q_r)^2 - mg_s q_r\cos(q_\theta)\right) - \frac{p_\theta^2}{q_r^2}} && (119)
\end{aligned}$$

where E_{ab} represents total mechanical energy during compression phase which is constant, $H_{ab}(q_r, q_\theta, p_r, p_\theta) = E_{ab}$.

Using Theorem 1 and Observation 1 and under reasonable assumptions ξ_x is found as in [10, Appendix A] for the following integrals.

$$\int_{q_{r_{td}}}^{q_r} \frac{1}{H_{ab}^{-1}(\sigma, q_\theta, p_\theta, E_{ab})} d\sigma \approx \frac{1}{H_{ab}^{-1}(\hat{\xi}_x, \hat{q}_\theta(\hat{\xi}_x), \hat{p}_\theta(\hat{\xi}_x), E_{ab})}(q_r - q_{r_{td}}) \quad (120)$$

$$\int_{q_{r_{td}}}^{q_r} \frac{1}{\sigma^2 H_{ab}^{-1}(\sigma, q_\theta, p_\theta, E_{ab})} d\sigma \approx \frac{1}{\hat{\xi}_x^2 H_{ab}^{-1}(\hat{\xi}_x, \hat{q}_\theta(\hat{\xi}_x), \hat{p}_\theta(\hat{\xi}_x), E_{ab})}(q_r - q_{r_{td}}) \quad (121)$$

$$\int_{q_{r_{td}}}^{q_r} \frac{\sigma}{H_{ab}^{-1}(\sigma, q_\theta, p_\theta, E_{ab})} d\sigma \approx \frac{\hat{\xi}_x}{H_{ab}^{-1}(\hat{\xi}_x, \hat{q}_\theta(\hat{\xi}_x), \hat{p}_\theta(\hat{\xi}_x), E_{ab})}(q_r - q_{r_{td}}) \quad (122)$$

where $\hat{\xi}_r$ is found for all of the integrals the same as

$$\hat{\xi}_x = \frac{3}{4} q_{r_{td}} + \frac{1}{4} q_r \quad (123)$$

Thus, nonlinear coupled differential equations (116),(117) and (118) can be solved iteratively as below and they are iterative approximate stance map equations for compression phase.

$$\hat{t}_{s_{(n+1)}}(q_r) = t_{td} - \frac{m}{H_{ab}^{-1}(\hat{\xi}_r, \hat{q}_{\theta_n}(\hat{\xi}_r), \hat{p}_{\theta_n}(\hat{\xi}_r), E)}(q_r - q_{r_{td}}) \quad (124)$$

$$\hat{q}_{\theta_{(n+1)}}(q_r) = q_{\theta_{td}} - \frac{\hat{p}_{\theta_n}(\hat{\xi}_r)}{\hat{\xi}_r^2 H_{ab}^{-1}(\hat{\xi}_r, \hat{q}_{\theta_n}(\hat{\xi}_r), \hat{p}_{\theta_n}(\hat{\xi}_r), E_{ab})}(q_r - q_{r_{td}}) \quad (125)$$

$$\hat{p}_{\theta_{(n+1)}}(q_r) = p_{\theta_{td}} - \frac{m^2 g_s \hat{\xi}_r \sin(\hat{q}_{\theta_n}(\hat{\xi}_r))}{H_{ab}^{-1}(\hat{\xi}_r, \hat{q}_{\theta_n}(\hat{\xi}_r), \hat{p}_{\theta_n}(\hat{\xi}_r), E_{ab})}(q_r - q_{r_{td}}) \quad (126)$$

$$\hat{p}_{r_{(n+1)}}(q_r) = -\sqrt{2m\left(E_{ab} - \frac{1}{2}k_c(l_0 - \hat{\xi}_r)^2 - m g_s \hat{\xi}_r \cos(\hat{q}_{\theta_{(n+1)}}(\hat{\xi}_r))\right) - \frac{\hat{p}_{\theta_{(n+1)}}^2(\hat{\xi}_r)}{\hat{\xi}_r^2}} \quad (127)$$

where n is the iteration number.

The zeroth iteration can be any approximate analytical solution for contact phase. In [10] three different initial approximate solutions are used and [3] may be a good initial iteration for this iterative approximation.

This approximate stance map is a good and valuable application of mean value theorem (Theorem 1). During derivations, g(t) is assumed to be always one and rest of the function inside the integral is considered as function f(t), where g(t) and f(t) are continuous functions described as in Theorem 1. For different f(t), different $\hat{\xi}_r$

is calculated and they are turned to be the same as in (123). For slightly different application of Theorem 1, $f(t)$ can be selected for all integrals as given below and $g(t)$ is rest of functions inside the integral which is the integrable part of the function;

$$f(t) = \frac{1}{H_{ab}^{-1}(t, q_\theta, p_\theta, E_{ab})}. \tag{128}$$

Hence the approximate solutions of integrals are given by

$$\int_{q_{r_{td}}}^{q_r} \frac{1}{H_{ab}^{-1}(\sigma, q_\theta, p_\theta, E_{ab})} d\sigma \approx \frac{1}{H_{ab}^{-1}(\hat{\xi}_x, \hat{q}_\theta(\hat{\xi}_x), \hat{p}_\theta(\hat{\xi}_x), E_{ab})}(q_r - q_{r_{td}}) \tag{129}$$

$$\int_{q_{r_{td}}}^{q_r} \frac{1}{\sigma^2 H_{ab}^{-1}(\sigma, q_\theta, p_\theta, E_{ab})} d\sigma \approx \frac{1}{H_{ab}^{-1}(\hat{\xi}_x, \hat{q}_\theta(\hat{\xi}_x), \hat{p}_\theta(\hat{\xi}_x), E_{ab})}(\frac{1}{q_{r_{td}}} - \frac{1}{q_r}) \tag{130}$$

$$\int_{q_{r_{td}}}^{q_r} \frac{\sigma}{H_{ab}^{-1}(\sigma, q_\theta, p_\theta, E_{ab})} d\sigma \approx \frac{1}{2H_{ab}^{-1}(\hat{\xi}_x, \hat{q}_\theta(\hat{\xi}_x), \hat{p}_\theta(\hat{\xi}_x), E_{ab})}(q_r^2 - q_{r_{td}}^2) \tag{131}$$

and $\hat{\xi}_r$ is found for approximate integral of $f(t)$ as below and it is the same as previous one because $f(t)$ is also one of the previous function inside the integral operator

$$\hat{\xi}_x = \frac{3}{4} q_{r_{td}} + \frac{1}{4} q_r. \tag{132}$$

Therefore, new iterative approximate stance map for compression phase is given by

$$\hat{t}_{s_{(n+1)}}(q_r) = t_{td} - \frac{m}{H_{ab}^{-1}(\hat{\xi}_r, \hat{q}_{\theta_n}(\hat{\xi}_r), \hat{p}_{\theta_n}(\hat{\xi}_r), E)}(q_r - q_{r_{td}}) \tag{133}$$

$$\hat{q}_{\theta_{(n+1)}}(q_r) = q_{\theta_{td}} - \frac{\hat{p}_{\theta_n}(\hat{\xi}_r)}{H_{ab}^{-1}(\hat{\xi}_r, \hat{q}_{\theta_n}(\hat{\xi}_r), \hat{p}_{\theta_n}(\hat{\xi}_r), E_{ab})}(\frac{1}{q_{r_{td}}} - \frac{1}{q_r}) \tag{134}$$

$$\hat{p}_{\theta_{(n+1)}}(q_r) = p_{\theta_{td}} - \frac{m^2 g_s \sin(\hat{q}_{\theta_n}(\hat{\xi}_r))}{2H_{ab}^{-1}(\hat{\xi}_r, \hat{q}_{\theta_n}(\hat{\xi}_r), \hat{p}_{\theta_n}(\hat{\xi}_r), E_{ab})}(q_r^2 - q_{r_{td}}^2) \tag{135}$$

$$\hat{p}_{r_{(n+1)}}(q_r) = -\sqrt{2m\left(E_{ab} - \frac{1}{2}k_c(l_0 - \hat{\xi}_r)^2 - m g_s \hat{\xi}_r \cos(\hat{q}_{\theta_{(n+1)}}(\hat{\xi}_r))\right) - \frac{\hat{p}_{\theta_{(n+1)}}^2(\hat{\xi}_r)}{\hat{\xi}_r^2}} \tag{136}$$

where n is the iteration number.

5.2.2 Bottom to Apex Map

Hamiltonian (total energy) function for the decompression phase is

$$H_{ba} = \frac{1}{2m}\left(p_r^2 + \frac{p_\theta^2}{q_r^2}\right) + \frac{1}{2}k_d(l_0 - q_r)^2 + mg_s q_r \cos(q_\theta) \tag{137}$$

inverse of Hamiltonian function is given by

$$H_{ba}^{-1}(q_r, q_\theta, p_\theta, E_{ba})\sqrt{2m\left(E_{ba} - \frac{1}{2}k_d(l_0 - q_r)^2 - mg_s q_r \cos(q_\theta)\right) - \frac{p_\theta^2}{q_r^2}} \tag{138}$$

where E_{ba} is total energy during compression phase at it is conserved. The relation between E_{ba} and E_{ab} is given by Eq.(98).

Approximate iterative bottom to apex map is given in [10] as

$$\hat{t}_{s_{(n+1)}}(q_r) = t_b + \frac{m}{H_{ba}^{-1}(\hat{\xi}_r, \hat{q}_{\theta_n}(\hat{\xi}_r), \hat{p}_{\theta_n}(\hat{\xi}_r), E_{ba})}(q_r - q_{r_b}) \tag{139}$$

$$\hat{q}_{\theta_{(n+1)}}(q_r) = q_{\theta_b} + \frac{\hat{p}_{\theta_n}(\hat{\xi}_r)}{\hat{\xi}_r^2 H_{ba}^{-1}(\hat{\xi}_r, \hat{q}_{\theta_n}(\hat{\xi}_r), \hat{p}_{\theta_n}(\hat{\xi}_r), E_{ba})}(q_r - q_{r_b}) \tag{140}$$

$$\hat{p}_{\theta_{(n+1)}}(q_r) = p_{\theta_b} + \frac{m^2 g_s \hat{\xi}_r \sin(\hat{q}_{\theta_n}(\hat{\xi}_r))}{H_{ba}^{-1}(\hat{\xi}_r, \hat{q}_{\theta_n}(\hat{\xi}_r), \hat{p}_{\theta_n}(\hat{\xi}_r), E_{ba})}(q_r - q_{r_b}) \tag{141}$$

$$\hat{p}_{r_{(n+1)}}(q_r) = \sqrt{2m\left(E_{ba} - \frac{1}{2}k_d(l_0 - \hat{\xi}_r)^2 - mg_s\hat{\xi}_r \cos(\hat{q}_{\theta_{(n+1)}}(\hat{\xi}_r))\right) - \frac{\hat{p}_{\theta_{(n+1)}}^2(\hat{\xi}_r)}{\hat{\xi}_r^2}} \tag{142}$$

where n is the iteration number and $\hat{\xi}_r$ is given by

$$\hat{\xi}_x = \frac{3}{4}q_{r_b} + \frac{1}{4}q_r \tag{143}$$

The zeroth iteration can be any approximate analytical solution for contact phase. In [10] three different initial approximate solutions are used and [3] may be a good initial iteration for this iterative approximation.

During the derivation of this iterative bottom to apex map, mean value theorem has significant role. If $f(t)$ and $g(t)$ is defined as in Theorem 1, in [10] $g(t)$ is always choose one and rest of the function in integral is represented by $f(t)$. For all nonlinear integral equations $\hat{\xi}_r$ is calculated and found to be the same for all ones as in (143).

For slightly different application of Theorem 1, $f(t)$ can be selected for all integrals as below and $g(t)$ is rest of functions inside the integral which is the integrable part of the function.

$$f(t) = \frac{1}{H_{ba}^{-1}(t, q_\theta, p_\theta, E_{ba})} \tag{144}$$

hence the approximate solutions of integrals are given by

$$\begin{aligned}
\int_{q_{r_b}}^{q_r} \frac{1}{H_{ba}^{-1}(\sigma, q_\theta, p_\theta, E_{ba})} d\sigma &\approx \frac{1}{H_{ba}^{-1}(\hat{\xi}_x, \hat{q}_\theta(\hat{\xi}_x), \hat{p}_\theta(\hat{\xi}_x), E_{ba})}(q_r - q_{r_b}) && (145)\\
\int_{q_{r_b}}^{q_r} \frac{1}{\sigma^2 H_{ba}^{-1}(\sigma, q_\theta, p_\theta, E_{ba})} d\sigma &\approx \frac{1}{H_{ba}^{-1}(\hat{\xi}_x, \hat{q}_\theta(\hat{\xi}_x), \hat{p}_\theta(\hat{\xi}_x), E_{ba})}(\frac{1}{q_{r_b}} - \frac{1}{q_r}) && (146)\\
\int_{q_{r_b}}^{q_r} \frac{\sigma}{H_{ba}^{-1}(\sigma, q_\theta, p_\theta, E_{ba})} d\sigma &\approx \frac{1}{2H_{ba}^{-1}(\hat{\xi}_x, \hat{q}_\theta(\hat{\xi}_x), \hat{p}_\theta(\hat{\xi}_x), E_{ba})}(q_r^2 - q_{r_b}^2) && (147)
\end{aligned}$$

and $\hat{\xi}_r$ is found for approximate integral of $f(t)$ as in (143) and it is the same as previous one because $f(t)$ is also one of the previous function inside the integral operator.

Therefore, new iterative approximate stance map for decompression phase is given by

$$\begin{aligned}
\hat{t}_{s_{(n+1)}}(q_r) &= t_b + \frac{m}{H_{ba}^{-1}(\hat{\xi}_r, \hat{q}_{\theta_n}(\hat{\xi}_r), \hat{p}_{\theta_n}(\hat{\xi}_r), E_{ba})}(q_r - q_{r_b}) && (148)\\
\hat{q}_{\theta_{(n+1)}}(q_r) &= q_{\theta_b} + \frac{\hat{p}_{\theta_n}(\hat{\xi}_r)}{H_{ba}^{-1}(\hat{\xi}_r, \hat{q}_{\theta_n}(\hat{\xi}_r), \hat{p}_{\theta_n}(\hat{\xi}_r), E_{ba})}(\frac{1}{q_{r_b}} - \frac{1}{q_r}) && (149)\\
\hat{p}_{\theta_{(n+1)}}(q_r) &= p_{\theta_b} + \frac{m^2 g_s \sin(\hat{q}_{\theta_n}(\hat{\xi}_r))}{2H_{ba}^{-1}(\hat{\xi}_r, \hat{q}_{\theta_n}(\hat{\xi}_r), \hat{p}_{\theta_n}(\hat{\xi}_r), E_{ba})}(q_r^2 - q_{r_b}^2) && (150)\\
\hat{p}_{r_{(n+1)}}(q_r) &= \sqrt{2m\left(E_{ba} - \frac{1}{2}k_d(l_0 - \hat{\xi}_r)^2 - m g_s \hat{\xi}_r \cos(\hat{q}_{\theta_{(n+1)}}(\hat{\xi}_r))\right) - \frac{\hat{p}_{\theta_{(n+1)}}^2(\hat{\xi}_r)}{\hat{\xi}_r^2}} && (151)
\end{aligned}$$

where n is the iteration number.

The general formulation of iterative apex return map for variable stiffness case is derived with one missing important parameter which is the bottom leg length, q_{r_b}. Bottom leg length is crucial since apex return map is divided into two parts (apex

to bottom and bottom to apex maps) around the bottom leg length. The general exact solution of the bottom length is not known, but several approximate solutions can be used. First one is symmetric gait assumption and exact bottom length can be calculated by using total energy relation since SLIP is verticular at bottom instance for symmetric gaits.

$$E_{ab} = \frac{p_\theta}{2mq_r^2} + \frac{k_c}{2}(l_0 - q_r)^2 + mg_s q_r \tag{152}$$

$$\frac{k_c}{2}q_r^4 + (mg_s - k_c l_0)q_r^3 + \left(\frac{k_c l_0^2}{2} - E_{ab}\right)q_r^2 + \frac{p_\theta^2}{2m} = 0 \tag{153}$$

(153) is a quartic equation of bottom leg length and one solution of this quartic equation which is real and less than or equal to the rest leg length gives the bottom leg length.

Another way of approximate calculation of bottom leg length is usage of approximate stance map in [3]. Approximate bottom leg length, q_{r_b}, is given by

$$q_{r_b} = l_0(1 + a_{ab} - b_{ab}) \tag{154}$$

where a_{ab} and b_{ab} are the same as in section 5.1.1.

6 Performance Analysis

Performance Analysis

6.1 Simulation Results

Simulation Results

7 Discussion

Discuss...

8 Conclusion

To sum up ...

References

[1] H. Benjamin Brown and Garth Zeglin. The bow leg hopping robot. In *Proceedings of the IEEE International Conference on Robotics and Automation*, Leuven, Belgium, May 1998.

[2] Sean Goodwin Carver. *Control of a spring-mass hopper*. PhD thesis, Ithaca, NY, USA, 2003. Adviser-John Guckenheimer.

[3] Hartmut Geyer, Andre Seyfartha, and Reinhard Blickhanb. Spring-mass running: simple approximate solution and application to gait stability. *Journal of Theoretical Biology*, 232:315 –328, February 2005.

[4] P. Holmes. Poincaré, celestial mechanics, dynamical-systems theory and "chaos". *Physics Reports (Review Section of Physics Letters)*, 193:137–163, September 1990.

[5] Marc H. Raibert. *Legged robots that balance*. Massachusetts Institute of Technology, Cambridge, MA, USA, 1986.

[6] Uluc Saranli. *Dynamic locomotion with a hexapod robot*. PhD thesis, Ann Arbor, MI, USA, 2002. Chair-Daniel E. Koditschek.

[7] Uluc Saranli and D. E. Koditschek. Template based control of hexapedal running. In *Proceedings of the IEEE International Conference On Robotics and Automation*, September 2003. accepted for publication.

[8] Uluc Saranli, William J. Schwind, and Daniel E. Koditschek. Toward the control of multi-jointed, monoped runner. In *Proceedings of the IEEE International Conference On Robotics and Automation*, pages 2676–2682, Leuven, Belgium, May 1998.

[9] William J. Schwind, Jun Ji, and Daniel E. Koditschek. A physically motivated further note on the mean value theorem for integrals. *The American Mathematical Monthly*, 106(6):559–564, June-July 1999.

[10] William J. Schwind and Daniel E. Koditschek. Approximating the stance map of a 2 dof monoped runner. *Journal of Nonlinear Science*, 10(5):533–588, 2000.

[11] William John Schwind. *Spring loaded inverted pendulum running: a plant model.* PhD thesis, Ann Arbor, MI, USA, 1998. Chair-Daniel E. Koditschek.

[12] E. T. Whittacker. *A treatise on the analytical dynamics of particles and rigid bodies, Fourth ed.* Cambridge University Press, New York, 1904.

[13] Garth Zeglin and H. Benjamin Brown. Control of a bow leg hopping robot. In *Proceedings of the IEEE International Conference on Robotics and Automation*, Leuven, Belgium, May 1998.